Available online at www.sciencedirect.com
SCIENCE DIRECT®
Polymer 44 (2003) 4673–4679
polymer
www.elsevier.com/locate/polymer

Growth process of homogeneously and heterogeneously nucleated spherulites as observed by atomic force microscopy

Yu-Guo Lei[a], Chi-Ming Chan[a,*], Yong Wang[a], Kai-Mo Ng[a,b], Yong Jiang[c], Li Lin[c,*]

[a]*Department of Chemical Engineering, Hong Kong University of Science and Technology, Clear Water Bay, Kowloon, Hong Kong*
[b]*Advanced Engineering Materials Facility, Hong Kong University of Science and Technology, Clear Water Bay, Kowloon, Hong Kong*
[c]*State Key Laboratory of Polymer Physics and Chemistry, Center for Molecular Science, Institute of Chemistry, Chinese Academy of Sciences, Beijing 100080, People's Republic of China*

Received 11 November 2002; received in revised form 18 February 2003; accepted 25 May 2003

Abstract

A poly(bisphenol A octane ether) (BA-C8) was synthesized. The isothermal spherulitic growth process was studied in situ using atomic force microscopy (AFM) at room temperature. For spherulites formed by homogeneous nucleation, the growth process includes the birth of a primary nucleus, the development of a founding lamella and the growth of the founding lamella into a spherulite. An embryo below a critical size is unstable. A stable embryo grows into a founding lamella. There is only one founding lamella in each spherulite. All other lamellae originate from this founding lamella. Two eyes can be seen at the center of a spherulite. For spherulites formed through heterogeneous nucleation, many lamellae grow at the nucleus surface and propagate outward radially. The spherulites acquire spherical symmetry at the early stage of crystallization. No eyes are found for this kind of spherulites.

Keywords: Atomic force microscopy; Homogeneous and heterogeneous nucleation; Polymer crystallization

1. Introduction

Spherulites are common crystalline structures observed in polymer systems [1,2]. Many studies have been performed to investigate their detailed structure and formation mechanism. The early studies performed using optical microscopy (OM) showed that a spherulite consisted of radiating fibrous crystallites [3,4]. Later, electron microscopy (EM) was used to study the lamellar morphology of spherulites. Phillips and Edwards studied the spherulitic morphology and growth kinetics of natural, isomerized, and synthetic *cis*-polyisoprene under different pressures with transmission electron microscopy (TEM) [5–12]. The polymer thin films were stained with osmium tetroxide vapor to stop the crystallization and enhance the phase contrast. Heterogeneous nucleation and homogeneous nucleation were both observed [7]. Heterogeneous nucleation was identified by the observations of lamellae growing in all directions normal to the surface of the nucleus. For homogeneous nucleation, lamellae were observed to grow in two directions. The growth rates of primary and subsidiary lamellae were found to be the same and constant [8]. The spherulitic morphologies of melt-crystallized, poly(4-methyl pentane) [13] polyethylene [14–17], isotactic polypropylene (*i*-PP) [18] and isotactic polystyrene [19] were investigated using OM and TEM. The main points made by the authors concerning the spherulitic growth were that dominant lamellae first grew into the melt to form a skeleton of a spherulite by splaying and branching; interdominant lamellar regions were filled with subsidiary lamellae; and branching was mainly through giant screw dislocations. The pressure built-up by molecular cilia between lamellae caused the splaying.

OM and EM have a wide range of applications in studies of polymer morphologies. However, they have a few drawbacks, making them unsuitable for application in real-time studies of spherulitic growth at lamellar level. For OM, the resolution was too low to detect lamellae. For scanning electron microscopy (SEM) and TEM, the required sample preparation techniques usually stop the crystal growth. The invention of atomic force microscopy

* Corresponding author. Tel.: +852-2358-7125; fax: +852-2358-7125.
E-mail address: kecmchan@ust.hk (C.M. Chan).

0032-3861/03/$ - see front matter © 2003 Elsevier Science Ltd. All rights reserved.
doi:10.1016/S0032-3861(03)00440-3

(AFM) provides a powerful technology for the investigation of polymer crystallization as the microscopy uses an easy sample preparation method, has high resolution and the ability to image dynamic processes at different temperatures [20–22]. With AFM, the spherulitic morphology and growth kinetics of various semi-crystalline polymers have been studied [23–28]. The three-dimensional view of an *i*-PP β-spherulite was obtained by Vansco and colleagues [23]. The results confirmed the observation of spherulitic morphology resolved by TEM. Hobbs and co-workers made a direct observation of the spherulitic growth of poly(hydroxybutyrate-*co*-valerate) using AFM [24]. They found that the overall growth rate was constant, while the individual lamella propagated with various rates. Recently, the melting and crystallization of polyethylene oxide [27–30], polyethylene terephthalate [31], polyethylene [32] and some other polymers [33–38] have been studied by AFM equipped with a hot stage.

In order to record the dynamic polymer crystal growth process in situ, two factors are significantly important. One is a technique with a very high resolution. It can repeatedly record the same area without damages to or significant interactions with the sample. AFM has been proved to be a successful tool to fulfill this task. The other key factor is that the polymers must have an appropriate crystallization rate. It generally takes an AFM several minutes to produce an image. This demands that the polymer has a very slow crystallization rate. The crystallization rates of most commercial polymers at room temperature are too fast.

It is well known that the crystallization rate and crystallinity of a polymer are strongly dependent on the crystallization temperature and polymer chain structure. A polymer can be controlled to have a slow crystallization rate by crystallizing at a high temperature close to its melting point or a lower temperature near its glass transition temperature. It is difficult to obtain high-quality AFM images for polymers at high temperatures because the melt may interact with the AFM tip which may induce crystallization as well. To run AFM at low temperatures, a cooler is required to keep the sample cool. As a result, the operation at or near room temperature is preferred. Modifying the polymer chain structure can reduce the crystallization rate. Varying the flexible segment length can control the flexibility of the polymer chain, which affects its crystallization rate significantly.

We synthesized a series of polymers (BA-Cn) by phase-transfer catalyzed polyetherification of 1, *n*-dibromoalkane ($n_1n = 4$, 6, 8, 10, 12, 14 and 18) with bisphenol A (BA), with a hard BA segment and a flexible Cn segment. The reaction and chemical structures have been described previously [39]. Our results indicated that poly(bisphenol A octane ether) (BA-C8) is one of the suitable candidates that has a slow crystallization rate at room temperature. The detailed spherulitic growth process of BA-C8 was clearly resolved by Li et al. [25,26]. Visualization of the isothermal crystallization process of BA-C8 thin films revealed several important features associated with the growth process of lamellae. The chain orientation was not as perfect at the growing lamellar tip as in other parts of the lamella. Hard tapping of an AFM tip twisted an edge-on lamella into a flat-on one. Branching was a result of the formation and growth of an induced nucleus at a location near the parent lamella. The lamellar growth rate was not constant. However, the crystallization rate of the polymer sample used was still too fast for the observation of the initial stage of crystallization, such as the birth of a primary nucleus and the development of the nucleus into a lamella because of its low molecular weight.

In a recent paper, we presented our observations on the initial stage of crystallization: the birth of a primary nucleus, the development of the first single lamella and the growth of lamellar sheaf. In this paper, we present detailed results on the growth process of homogeneously nucleated and heterogeneously nucleated spherulites.

2. Experiments

BA-C8 was synthesized by condensation polymerization of bisphenol A and 1,8-dibromoctane [39]. The glass transition temperature, melting point, number-average molecular weight, and polydispersity index of the polymer were 10.5, 83.3 °C, 13,750 g/mol, and 2.4, respectively. Thin BA-C8 polymer films were prepared by spin-coating a 30 mg ml^{-1} polymer–chloroform solution onto silicon wafers (~10 mm × 10 mm) at 4000 rpm. The samples were dried in a vacuum oven at room temperature for 30 min. The thickness of the amorphous BA-C8 films was estimated by a profilometer to be approximately 300 nm.

Tapping-mode AFM images were obtained under ambient conditions using a NanoScope III A MultiMode AFM with a hot-stage accessory (Digital Instruments). Both height and phase images were recorded simultaneously. Si tips (TESP) with a resonance frequency of approximately 300 kHz and a spring constant of about 40 N m^{-1} were used, and the scan rate was 0.8 Hz. The scanning density was 512 lines/frame. A set-point amplitude ratio of 0.8 was used. The phase contrast imaging technique was utilized to distinguish between the amorphous and crystalline phases.

3. Results and discussion

3.1. Homogeneous nucleation

3.1.1. Birth of primary nuclei

In a previous paper [40], we observed embryos appearing as 10 nm dots and some disappearing several minutes later. The results demonstrate that an embryo below a critical size may disintegrate. Fig. 1 shows a series of AFM phase images of the same area obtained at 22 °C. The image area was 1.6 μm × 1.6 μm and the time interval between two

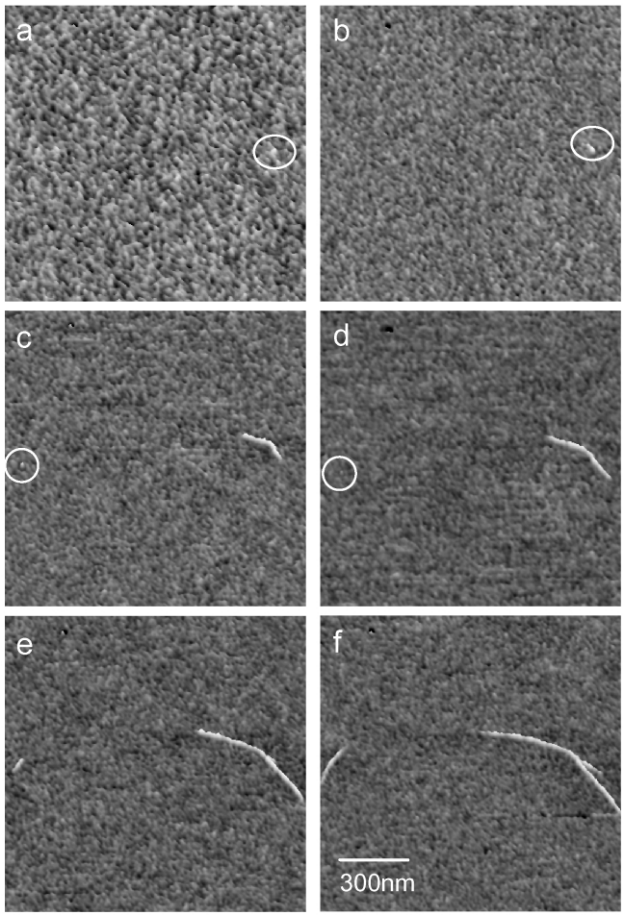

Fig. 1. Phase images show the birth of a primary nucleus and development of the founding lamella. The time interval between the images was 10.6 min.

successive images was 10.6 min. An embryo can be seen in the middle of the right side of Fig. 1(a). This embryo has two growing fronts where polymer chain segments fold into the crystal lattice. Eventually, this embryo grows into a founding lamella (Fig. 1(b) and (c)).

Another embryo can be found in the middle at the left side of Fig. 1(c). This embryo appears to disintegrate 10.6 min later as no embryo has been detected at the same location, as shown in Fig. 1(d). However, this disintegration is not complete. As a result, a new embryo appears again at the same place (Fig. 1(e)). In summary, an embryo below a critical size is not stable. It can disintegrate. Sometimes an embryo completely disintegrates into amorphous materials as observed previously [25,40,41]. Sometimes this disintegration is not complete and an embryo may appear at the same location.

3.1.2. Development of the founding lamella

Once an embryo grows larger than the critical size as predicted by thermodynamics, it can grow continuously at both ends and develop into a single lamella, as shown in a series of images (Fig. 1). The embryo, as shown in Fig. 1(b), keeps growing at both growing tips and develops into a founding lamella (Fig. 1(c)). The founding lamella is about 0.8 μm long before induced nucleation occurs (Fig. 1(e)).

There is a concern that the AFM tip can induce the growth of the founding lamella in the direction normal to the fast scanning direction of the AFM tip. Fig. 2 shows three AFM phase images obtained at 25 °C. The image area was 1.5 μm × 1.5 μm. The fast scanning direction was horizontal with respect to the image while the slow scanning direction was vertical. It is clear that the growth direction of these founding lamellae is independent of the fast scanning direction. These results indicate that for light tapping, the AFM tip scanning direction has no effect on the growth direction of the lamellae.

3.1.3. Growth of spherulites

Fig. 3 shows AFM phase images obtained at 30 °C for the formation of a lamellar sheaf. The time interval between the images shown in Fig. 3 was 10.6 min. A founding lamella is clearly shown in Fig. 3(a). This founding lamella grows in

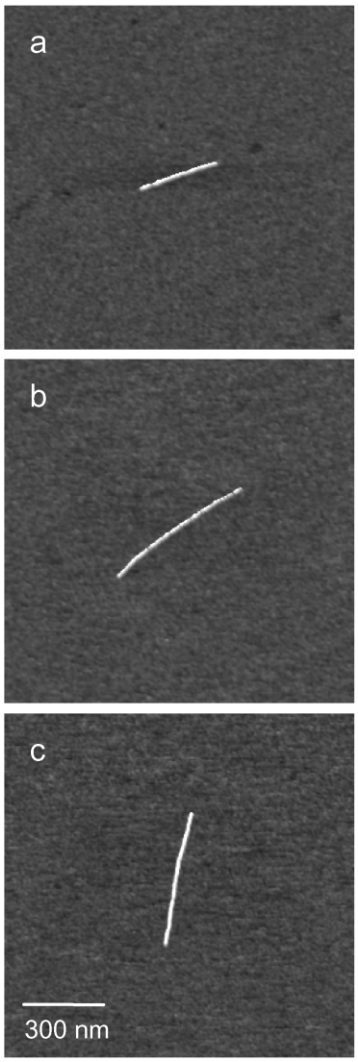

Fig. 2. Phase images show the founding lamellae growing in various directions with respect to the fast scanning direction of AFM.

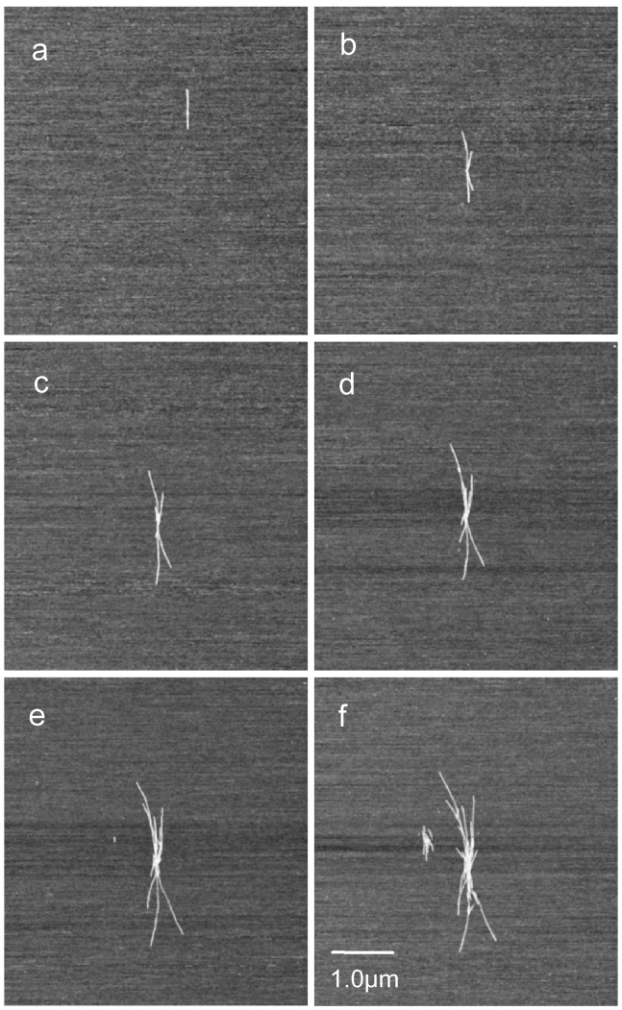

Fig. 3. Phase images show the growth of a lamellar sheaf. The time interval between the images was 10.6 min.

two directions. Branching occurs in the middle of the founding lamella. An induced nucleus formed next to the founding lamella, developed into a subsidiary lamella (Fig. 3(b)). This subsidiary lamella then grows both forward and backward. Another subsidiary lamella is formed at the left side of the founding lamella (Fig. 3(c)). Branching and splaying continue (Fig. 3(e)). Finally, a founding lamella grows into a lamellar sheaf (Fig. 3(f)), consisting of many lamellae.

Fig. 4 displays a series of AFM phase images obtained at 30 °C showing the development of a lamellar sheaf into a spherulite. A lamellar sheaf finally develops into a spherulite through branching and splaying. Fig. 4 also shows the formation of a pair of eyes at the center of the spherulite. A higher resolution phase image of the eyes for another sample obtained at 30 °C reveals that the eyes consist of only the flat-on lamellae, as shown in Fig. 5. One possible explanation is that as the edge-on lamellae start to propagate along the perimeter of the eyes, the strain energy increases due to the bending of the lamellae, as shown in Fig. 4(d)–(f). In order to propagate in a lower energetic

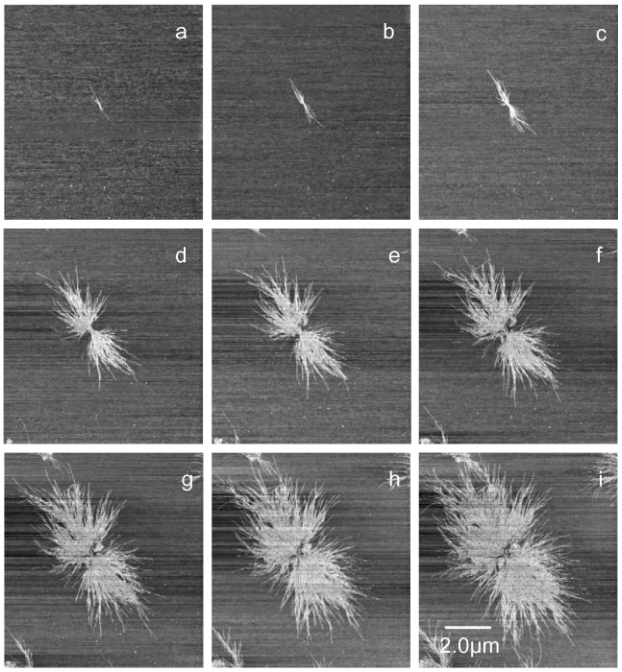

Fig. 4. Phase images show the growth of a spherulite. The time interval between the images was 14.2 min except that between c and d was 53 min.

state, flat-on lamellae become the preferred orientation because they can fill up the space in the eyes without causing any bending of the lamellae. The diameter of the eyes typically ranges between 1 and 2 μm.

3.1.4. Lamellar growth rate at the early stage of crystallization

The growth rate is important for any kinetic study. Many studies have been performed to measure the growth rate of spherulites using OM and recently AFM. It has been predicted by theoretical models and observed experimentally that the overall spherulitic growth rate is constant. As for an individual lamellar growth rate, Hobbs pointed out that some lamellae initially grew forward faster than the overall growth rate of spherulites [24]. And the growth rate

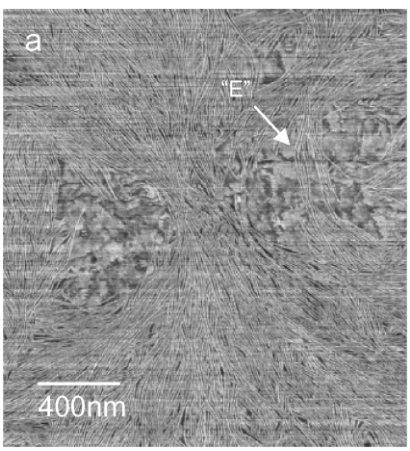

Fig. 5. Phase image shows the structure of the eyes.

was not constant. It varied for different lamellae, and even for the same lamellae at different locations [24]. In our earlier work, we also observed that a lamella might propagate faster in the forward direction than the overall growth rate. We saw that the propagation could slow down or even stop for a period of time and then restart again [26].

To study the growth rate of the lamellae, their lengths were measured as a function of time at 22 °C. The length of a founding lamella (lamella 1) and a subsidiary lamella (lamella 2) as a function of time is shown in Fig. 6. The growth rates of the founding and subsidiary lamellae were determined to be about 19 and 9 nm/min, respectively, from the slopes of the two straight lines in Fig. 6. It is important to note that the growth rate of the founding lamella is twice that of the subsidiary lamella because the founding lamella has two growing tips and the subsidiary lamella has only one. For convenience, we define the growth rate of lamellae to be approximately 9.5 nm/min at 22 °C, using the growth in one direction only. The growth rate of all lamellae was found to be quite uniform. Such results seem to be contradictory to those of the earlier observations [24,26]. But it should be noted that the earlier observations were made at different stages of the formation of spherulites (in the middle stage of the formation of the spherulites) while the present observation was made at the initial stage of the formation of the spherulites. Together, these results clearly indicate that the growth rate of the lamellae is different at different stages during the formation of the spherulites. The difference should reflect the influence of the concentration of growing lamellae on the growth rate of the lamellae.

At the middle stage of the formation of spherulites, there is a high concentration of growing lamellae. Furthermore, the size of a random coil of a polymer chain is far larger than the thickness of a lamella; consequently, many trapped chains should be present. These factors should play an important role affecting the growth rate of the lamellae. Furthermore, because the concentration of the growing lamellae is not uniform across the film, the growth rate should also vary significantly even for the same lamella. However, at the initial stage of the formation of the spherulites, the concentration of trapped polymer chains is low and the time needed for the chain segments to adjust their conformation to fit into the lattice is affected mainly by the original orientation of the chains. Hence, the variation of the growth rate among the lamellae is small.

To explore the effect of temperature on the growth rate of the lamellae, the length of the lamellae was measured at two other temperatures (16 and 28 °C) and the results are shown in Fig. 7. The growth rate of the lamellae at 16 and 28 °C was measured to be 8.2 and 32.4 nm/min, respectively. It increases significantly as the temperature increases indicating that the growth rate of the lamellae at this temperature range is limited by the diffusion of the polymer chains.

3.2. Heterogeneous nucleation

The previous sections described the growth process of spherulites induced by homogeneous nucleation. Heterogeneous nucleation, which can be identified by observation of lamellae growing in radial directions normal to the surface of the nucleus [7], was also studied. Fig. 8 is a series of phase images showing heterogeneous nucleation and the spherulitic growth process. The images, which were 10 μm × 10 μm in size, were taken at 30 °C. Fig. 8(a) shows six edge-on lamellae growing normal to the surface of a nucleus. More edge-on lamellae continue to develop at the nucleus surface and grow outward radially (Fig. 8(b)).

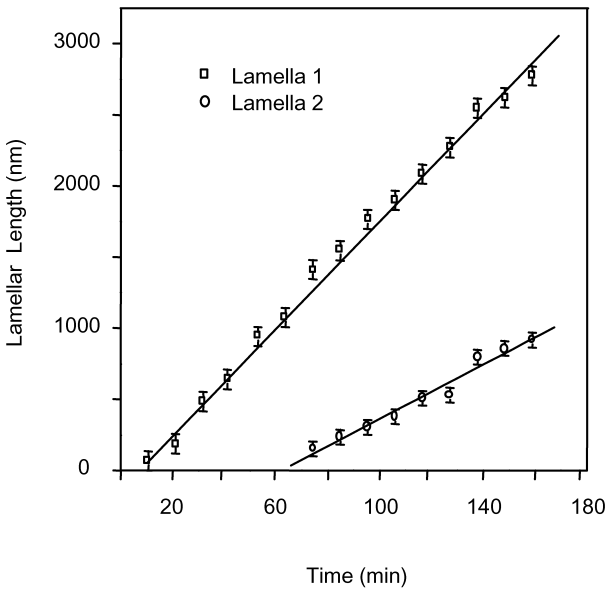

Fig. 6. Plots of the length of founding and secondary lamellae as a function of time at 22 °C.

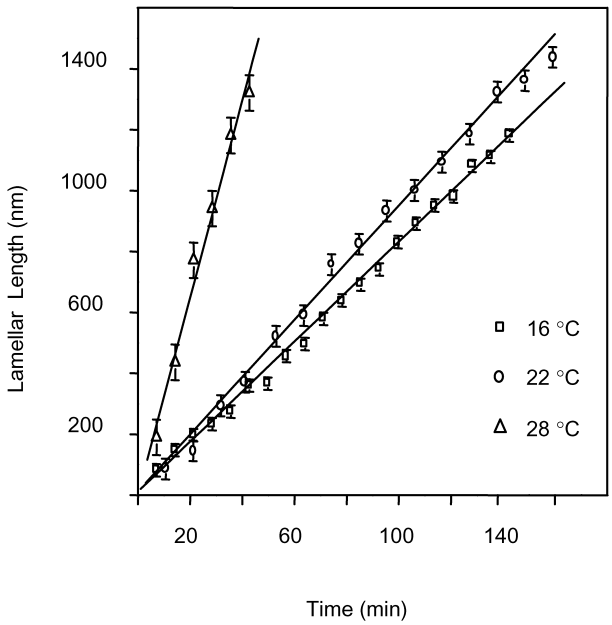

Fig. 7. The lengths of founding lamellae as a function of time measured at three different temperatures.

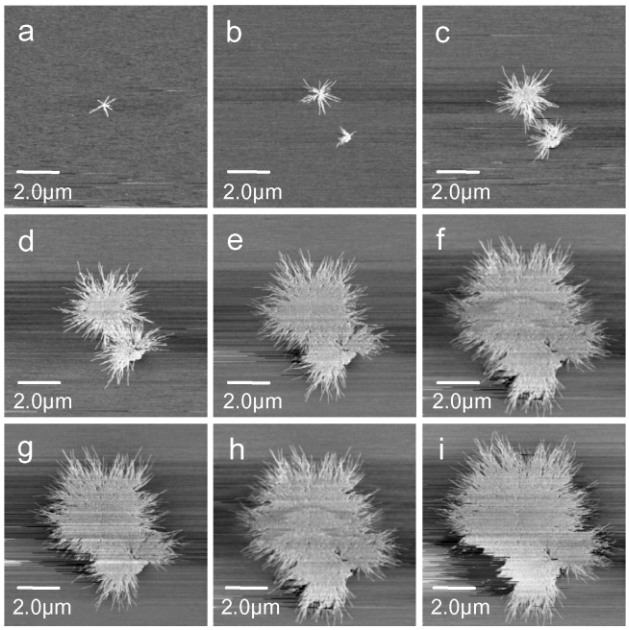

Fig. 8. Phase images show that growth of a heterogeneously nucleated spherulite. The time interval between the images was 14.8 min.

Subsidiary lamellae develop from induced nuclei (Fig. 8(c)). Branching and splaying continue, eventually a small spherulite is formed (Fig. 8(d)). Another spherulite formed as a result of homogeneous nucleation, can be seen at the lower right side of the heterogeneously nucleated spherulite.

The structure of this kind of heterogeneously nucleated spherulites is different from the homogeneously nucleated spherulites. First, for a heterogeneously nucleated spherulite, several lamellae can simultaneously develop on the surface of the nucleus. For a homogeneously nucleated spherulite, only one founding lamella is developed from a primary nucleus and all other lamellae are subsidiary lamellae originating from the founding lamella. For a heterogeneously nucleated spherulite, all lamellae grow into the melt in a direction normal to the nucleus surface. As a result, the spherulite has spherical symmetry starting even at the very early stage. No lamellar sheaf is seen. Consequently, the spherulites do not have a pair of eyes at their center.

Fig. 8(g)–(i) shows the impingement of two spherulites. It is interesting to note that the boundary is formed by the interpenetration of lamellae from the two spherulites. These results suggest that the spherulitic growth process can significantly affect mechanical properties of semi-crystalline polymers. A detailed study on the effect of the spherulitic growth conditions on the mechanical properties will be presented in a forthcoming paper.

4. Conclusions

Spherulites formed by both homogeneous and heterogeneous nucleation were observed. A homogeneously nucleated spherulite started with a nucleus which developed into a founding lamella with polymer chain segments folding into the crystal lattice at two growing fronts. Through branching and splaying, subsidiary lamellae developed and grew and finally a spherulite with two characteristic eyes at the center was formed. For a heterogeneously nucleated spherulite, many lamellae grew at the surface of a heterogeneous nucleus and propagated outward radially. The spherulite acquired spherical symmetry at the every early stage of the crystallization process. Through branching and splaying a heterogeneously nucleated spherulite was formed and because of the formation process, which was different from that of a homogeneously nucleated spherulite, no eyes were found at the center of the spherulite.

Acknowledgements

This work was supported by the National Science Foundation of China and the Hong Kong Government Research Grants Council Joint Research Scheme under Grant No. N_HKUST 618/01 and the National Science Foundation of China under grant number 20131160730 as well as the Hong Kong Government Research Grants Council under grant number HKUST6176/02P.

References

[1] Bassett DC. Principles of polymer morphology. New York: Cambridge University Press; 1981.
[2] Woodward AE. Atlas of polymer morphology. New York: Hanser; 1988.
[3] Keller A. J Polym Sci 1955;17:291.
[4] Keith HD, Padden FJ. J Polym Sci 1959;39:101.
[5] Phillips PJ, Andrews EH. Polym Lett 1972;10:321.
[6] Phillips PJ, Edwards BC. J Polym Sci, Polym Phys Ed 1975;13:1819.
[7] Edwards BC, Phillips PJ. J Polym Sci, Polym Phys Ed 1975;13:2117.
[8] Phillips PJ, Edwards BC. Polym Lett Ed 1976;14:449.
[9] Phillips PJ, Sorenson D. J Polym Sci, Polym Phys Ed 1979;17:521.
[10] Edwards BC, Phillips PJ, Sorenson D. J Polym Sci, Polym Phys Ed 1980;18:1737.
[11] Phillips PJ, Sorenson D. J Polym Sci, Polym Lett Ed 1981;19:585.
[12] Rensch GJ, Phillips PJ, Vatansever N. J Polym Sci, Polym Phys 1986; 24:1943.
[13] Daxaben P, Bassett DC. Phil Trans R Soc Lond 1994;A445:577.
[14] Bassett DC, Olley RH, Al Raheil IAM. Polymer 1988;29:1539.
[15] Bassett DC. Phil Trans R Soc Lond 1994;A348:29.
[16] Bassett DC, Hodge AM. Proc R Soc Lond A 1981;A377:61.
[17] Bassett DC, Hodge AM. Proc R Soc Lond A 1981;A377:25.
[18] Bassett DC, Vaugham AS. Polymer 1985;26:717.
[19] Bassett DC, Olley RH. Polymer 1984;25:935.
[20] Magonov SN, Elings V, Whangbo MH. Surface Sci 1997;375:L385.
[21] Bar G, Thomann Y, Brandsch R, Cantow HJ, Whangbo MH. Langmuir 1997;13:3807.
[22] Bar G, Delineau L, Brandsch R, Bruch M. Appl Phys Lett 1999;25: 4198.
[23] Honeringen DT, Varga J, Ehrenstein GW, Vansco GJ. J Polym Sci, Polym Phys 2000;38:672.

[24] Hobbs JK, Mcmaster TJ, Miles MJ, Barham PJ. Polymer 1998;39: 2437.
[25] Li L, Chan CM, Li JX, Ng KM, Yeung KL, Weng LT. Macromolecules 1999;32:8240.
[26] Li L, Chan CM, Yeung KL, Li JX, Ng KM, Lei YG. Macromolecules 2001;34:316.
[27] Pearce R, Vansco GJ. Macromolecules 1997;30:5843.
[28] Pearce R, Vansco GJ. Polymer 1998;39:1237.
[29] Pearce R, Vansco GJ. J Polym Sci, Polym Phys 1998;36:2643.
[30] Beekmans LGM, Van der Meer DW, Vansco GJ. Polymer 2002;43: 1887.
[31] Ivanov DA, Amalou Z, Magonov SN. Macromolecules 2001;34:8944.
[32] Godovsky YK, Magonov SN. Langmuir 2000;16:3549.
[33] Kikkawa Y, Abe H, Iwata T, Inoue Y, Doi Y. Biomacromolecules 2001;2:940.
[34] Hobbs JK, Miles MJ. Macromolecules 2001;34:353.
[35] Hobbs JK, Humphris ADL, Miles MJ. Macromolecules 2001;34: 5508.
[36] Ivanov DA, Jonas AM. Macromolecules 1998;31:4546.
[37] Schultz JM, Miles MJ. J Polym Sci, Polym Phys 1998;36:2311.
[38] Ivanov DA, Nysten B, Jonas AM. Polymer 1999;40:5899.
[39] Li L, Chan CM, Ng KM, Weng LT. Polymer 2001;42:6841.
[40] Lei YG, Chan CM, Li JX, Ng KM, Wang Y, Jiang Y, Li L. Macromolecules 2002;35:6751.
[41] Schonherr H, Waymouth RM, Frank CW. Macromolecules 2003;36: 2412.